International Journal of Concrete Structures and Materials
Vol.11, No.2, pp.327–341, June 2017
DOI 10.1007/s40069-017-0186-7
ISSN 1976-0485 / eISSN 2234-1315

Strengthening of Cutouts in Existing One-Way Spanning R. C. Flat Slabs Using CFRP Sheets

Hamdy K. Shehab, Ahmed S. Eisa*, and Kareem A. El-Awady

(Received September 11, 2016, Accepted January 31, 2017, Published online June 1, 2017)

Abstract: Openings in slabs are usually required for many different applications such as aeriation ducts and air conditioning. Opening in concrete slabs due to cutouts significantly decrease the member stiffness. There are different techniques to strengthen slabs with opening cutouts. This study presents experimental and numerical investigations on the use of Carbon Fiber Reinforced Polymers (CFRP) as strengthening material to strengthen and restore the load carrying capacity of R.C. slabs after having cutout in the hogging moment region. The experimental program consisted of testing five (oneway spanning R.C. flat slabs) with overhang. All slabs were prismatic, rectangular in cross-section and nominally 2000 mm long, 1000 mm width, and 100 mm thickness with a clear span (distance between supports) of 1200 mm and the overhang length is 700 mm. All slabs were loaded up to 30 kN (45% of ultimate load for reference slab, before yielding of the longitudinal reinforcement), then the load was kept constant during cutting concrete and steel bars (producing cut out). After that operation, slabs were loaded till failure. An analytical study using finite element analysis (FEA) is performed using the commercial software ANSYS. The FEA has been validated and calibrated using the experimental results. The FE model was found to be in a good agreement with the experimental results. The investigated key parameters were slab aspect ratio for the opening ratios of [1:1, 2:1], CFRP layers and the laminates widths, positions for cutouts and the CFRP configurations around cutouts.

Keywords: cutouts, flat slab, reinforced concrete, strengthening, CFRP, bonding, line loads, numerical analysis.

1. Introduction

The ACI 318-14 code allows reinforced concrete slabs to have openings with the condition of performing full structural analysis to assure slab safety, strength, and serviceability under different expected loads. Whereas the ACI 318-14 (ACI 318-14) Code gives procedures and limits for opening location and size. If designer satisfies those requirements the analysis could be abandoned, hence, problem becomes more complex when openings are planned to be made in existing slab, the most common way to substitute additional steel reinforcement is to apply CFRP strengthening before cutting a hole. The ACI 318-14 (ACI 318-14) recommends the size and location of openings in two-way slab systems as shown in Fig. 1.

Today, the use of carbon fiber reinforced polymers (CFRP) as external reinforcement to strengthen existing slabs due to openings is becoming more popular, partly due to ease of installation and partly due to space saving. In these situations, CFRP sheets are applied to the slab before the opening is made even though CFRP is used for strengthening of openings, very few studies on the structural behavior of slabs with openings have been carried out. Casadei et al. (2003) ANSYS (2011) reported a series of tested one-way slabs with openings strengthened with CFRP. The slabs had openings at the centers and in areas close to the supports. Most of the reported work was related to the strengthening of slab openings at the positive moment regions. It was found that the presence of openings in the negative moment areas usually increases the shear stresses (Casadei et al. 2003). Tan and Zhao (2004) performed a study incorporated strengthened slabs with symmetric and asymmetric openings. The strengthened slabs showed equal or higher capacity of the control slabs with openings. Most of the slabs showed flexural failure mode whereas some of them showed a different failure pattern where the cracks extended from the opening corners. One of the Tan et al. (2004) findings was related to the failure mode dependency on the opening location. Slabs with openings placed in the maximum moment region failed in flexural mode while openings located in the shear region failed in shear mode.

Enochsson et al. (2007) tested two-way slabs strengthened with CFRP and the results showed that the stiffness and ultimate load of the slabs with large opening is higher than the small opening with the same opening locations. Those results could be attributed to the equivalency of larger slabs to hidden beams (Enochsson et al. 2007). Mota and Kamara (2006) presents a particularly detailed review of forming cutouts in two-ways slab systems. A lower-bound analytical model provided herein serves as an alternative form of

Structural Engineering Department, Faculty of Engineering, Zagazig University, Zagazig, Egypt.
*Corresponding Author; E-mail: ahmedeisa@zu.edu.eg

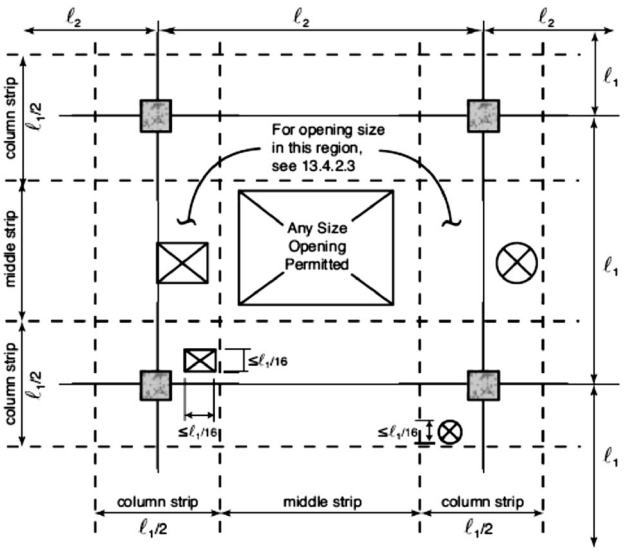

Fig. 1 Opening sizes and locations in flat plates (ACI 318-14).

practical analysis of FRP-strengthened slabs with cutouts. In addition, it considers the FRP effect and associated failure modes. The analytical method is essentially a strip method of analysis, and is based upon the ultimate moment of resistance provided by the slab along critical crack lines in any direction It considers longitudinal and transverse slab behavior, and is found to correlate well with existing and current test data provided certain assumptions are made for the calculation of the sectional strength and position of the critical crack.

Vasquez and Karbhari (2003) showed that the appropriate design of the strengthening measure enables capacity reduced by the presence of the cutout to be regained while mitigating and retarding crack growth. Ultimate failure was through a sequence of cracking and debonding of the FRP composite reinforcing strips with a decrease in load capacity after debonding to the response level of the unstrengthened slab with a cutout after yield of the steel reinforcement. More information about reinforced concrete slabs with cutouts strengthening could be found in Mosallam and Mosalam (2003), Ozgur et al. (2013).

Muhammed (2012), tested eight self-compacting concrete slabs. Results showed that, the use of CFRP strips is more effective than the steel fiber, use of steel fiber increased the load capacity by 26.67 and 9.83% for small and large opening respectively, while CFRP increased the load capacity by 46.67 and 55.7% for small and large opening respectively, CFRP and steel fiber reduced the cracks at the inside faces of the opening while CFRP prevent it at the inside corners of opening. Smith and Kim (2009) reported the results of strengthened one-way slabs with FRP cutouts at their centers. Four slabs with cutouts were tested in addition to two slabs without cutouts. The effect of different load application positions was investigated, in addition to distribution of stresses around the cutout. All FRP-strengthened slabs failed by de-bonding, however, the extent of de-bonding and the ability of the slab to sustain load post-initiation of de-bonding was dependent on the position of the load. The slab in which the line load was located adjacent to the cutout exhibited transverse bending action and as a result was able to withstand more extensive de-bonding prior to loss of load-carrying enhancement from the FRP.

Sorin-Codrut et al. (2015) studied two-way simply supported reinforced concrete slabs subjected to a uniformly distributed load. Slabs with strengthened and non-strengthened openings have been investigated. CFRP sheets have been used for the strengthening. Focusing on examining the structural behavior of two-way RC slabs strengthened with CFRP due to a sawn-up opening, test results clearly showed that the investigated strengthening system can be used to strengthen existing slabs with made openings, and even that the load carrying capacity can be increased when compared to the homogeneous slab, The slabs with the larger openings have a noticeable higher load carrying capacity and a stiffer load–deflection response than the slabs with the smaller openings. In addition to that, it was stated that the ultimate load of strengthened slabs with the cutouts increased by 121%.

The existence of openings in slabs can also degrade the in-plane capacity and stiffness of when they are subjected to in-plane/earthquake loads. Khajehdehia and Panahshahib (2016) conclude that that presence of openings clearly changed the in-plane behavior of RC slabs compared to those of slabs without openings and that this oversimplification in design and analysis of slabs by ignoring the opening effects might lead to erroneous results, Song et al. (2012). Tested three isolated interior flat slab-column connections that include three types of shear reinforcement details; stirrup, shear stud and shear band were tested under reversed cyclic lateral loading to observe the capacity of slab-column connections. The results were applied to the eccentricity shear stress model presented in ACI 318-08. The failure mode was defined by considering the upper limits for punching shear and unbalanced moment. In addition, an intensity factor was proposed for effective widths of slabs that carry an unbalanced moment delivered by bending.

The main aim of this study is to investigate the behavior of reinforced concrete one-way flat slabs with cutouts. The cutouts were made during slab loading which represents slabs under service conditions. The data generated in this paper are mainly came out of testing five slabs experimentally under various key parameters and by using finite element modeling.

2. Experimental Program

2.1 Description of Tested Slabs

The experimental program consisted of testing five (one-way spanning R.C. slabs) with an overhang. All slabs were prismatic, rectangular in cross-section and nominally 2000 mm long × 1000 mm width × 100 mm thickness with a clear span (distance between supports) of 1200 mm and a cantilever 700 mm long. All slabs were reinforced with 10 mm diameter steel bars top and bottom spaced at 160 mm

Table 1 Description of tested specimens.

Group	Specimen	Cutout aspect ratio	Cutout size (mm)	Use of CFRP sheets
Reference	S0	None	None	None
1	S1	1:1	200 × 200	None
	S2	2:1	200 × 400	None
2	S3	1:1	200 × 200	Around cutout at tension surface
	S4	2:1	200 × 400	Around cutout at tension surface

in both directions. Description and details of tested specimens are listed and shown in Table 1 and Fig. 2, respectively.

2.2 Materials

In this study, locally produced materials are used in all concrete mixtures, coarse and fine aggregates are composed of harsh desert sand, free from impurities, crushed dolomite from Ataka near Seuz Canal zone, ordinary Portland cement locally produced, and tap drinking water. High-grade steel locally produced was used as reinforcement; tests were carried out to determine the properties of the used materials according to the ASTM standard specifications. The characteristics of the strengthening materials (CFRP sheets and its impregnating resin) were taken from the manufacturing company product data sheets as well as the instructions of the installation process. Tables 2 and 3 show the mechanical properties of steel bars and the CFRP used in this study. Concrete cubes were taken from all mixtures to track the concrete compressive strength. The results of the tested control cubes for the concrete mix reached the required compressive strengths = 31 N/mm^2 at 28-days.

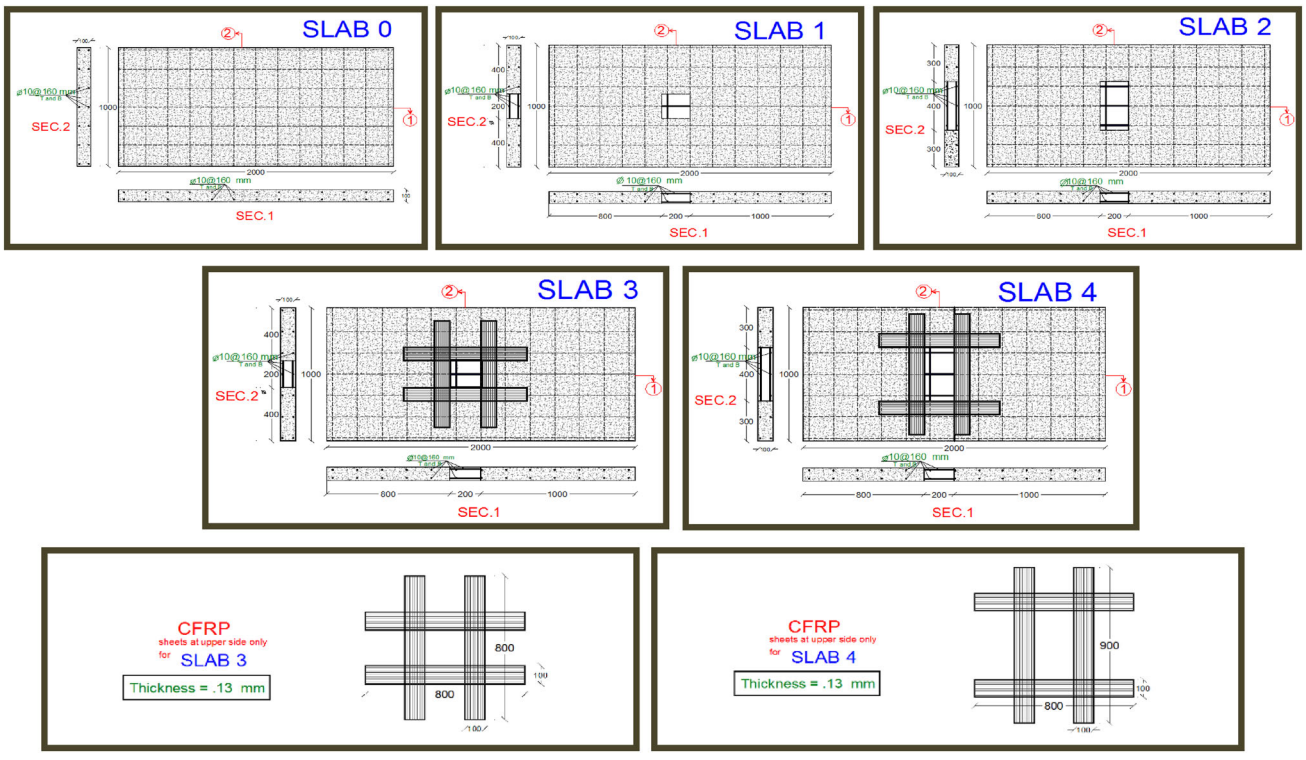

Fig. 2 Details of tested specimens.

Table 2 Mechanical properties of steel bars.

Nominal diameter (mm)	Yield load (kN)	Ultimate load (kN)	Yield stress (N/mm^2)	Ultimate tensile strength (N/mm^2)	Ultimate strain (%)
10	35.5	47.8	450	610	16

Table 3 Physical and mechanical properties of Sikawrap Hex®-230C.

Sikawrap Hex®-230C properties	
Areal weight (±10)	230 ± 10 (g/m^2)
Density	1.76 (g/cm^3)
Adhesive strength on concrete	4 (MPa)
Density	1.31 (Kg/lit)
CFRP unidirectional properties	
Tensile strength of fibers (nominal)	4300 (MPa)
Tensile E-modulus of fibers (nominal)	238,000 (MPa)
Strain at break of fibers	1.8 (%)
Fabric design thickness	0.13 (mm)
Tensile strength	30 (MPa)
Tensile E-modulus in flexural	3800 (MPa)

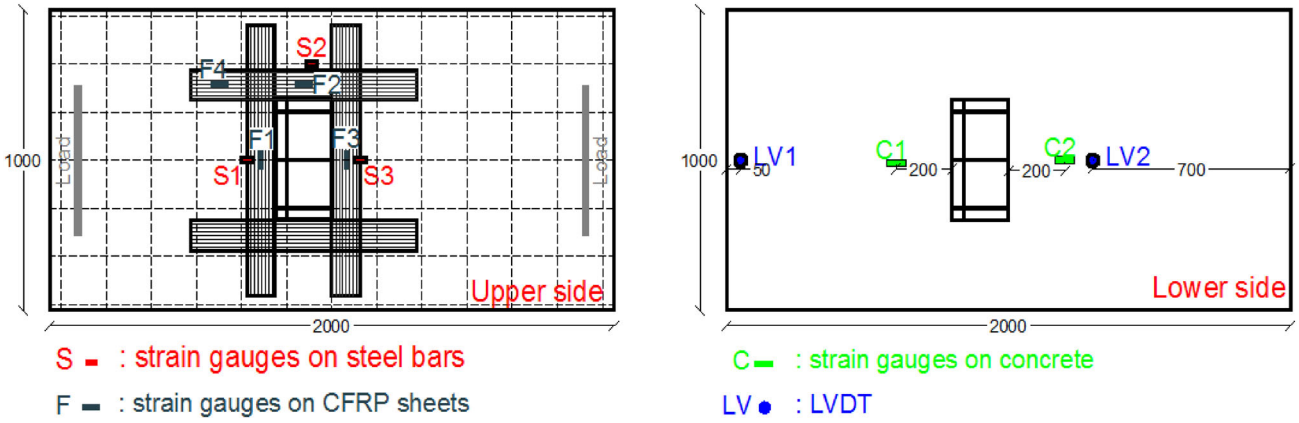

Fig. 3 Measuring instruments (strain gages and LVDTs) on the sides of the tested slabs.

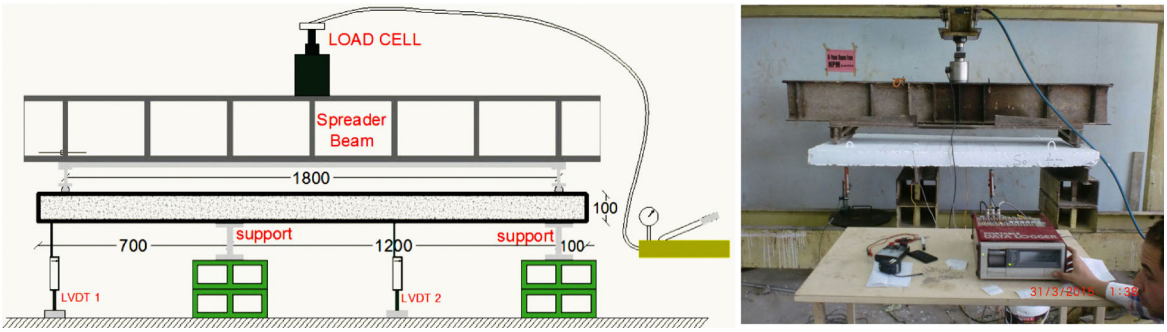

Fig. 4 Loading arrangement and test setup.

2.3 Sensors and Measurements

The specimens were instrumented to record the strains of concrete, steel bars and CFRP sheets as well. The load and deflection of all specimens were instrumented. The strain gages data were collected using a data logger system. Three electrical strain gages (S1, S2, and S3) were installed on top layer steel bars and two on the bottom concrete surface; strain gages (C1 and C2) as shown in Fig. 3. Four electrical strain gages were installed on top surface of the CFRP sheets, strain gages (F1, F2, F3, and F4), two in the longitudinal direction and the other two on the transverse direction. Deflection was measured using Linear Variable Distance Transducers (LVDT). Two LVDTs were installed on the lower side of each slab (LV1 and LV2).

2.4 Loading Arrangement and Test Procedure

All slabs were tested using a hydraulic machine of 25 ton capacity under three-point bending, the load was applied using a spreader I-beam as shown in Fig. 4. The spreader beam distributes this load on two rigid steel Sects. (500 mm long) as shown in Fig. 4. All slabs were loaded up to 30 kN service load (45% of ultimate load for reference slab, and before reaching the steel yielding stress) and that load was kept constant. While the service load was applied constantly, the opening were made at the predefined locations and with the designed sizes as shown in Fig. 5, after that, the load was increased till failure.

Fig. 5 Cutting concrete and steel bars.

3. Experimental Results and Dissusion

3.1 Flexural Failure Mode

The modes of failure of the tested slabs are listed in Table 4, and the crack patterns are shown in Fig. 6. Two modes of failure were observed during the tests; the control slab had a cracks parallel to the support line and at the maximum negative moment region and experienced flexural failure. Slabs S1 and S2 showed initially flexural cracks occurred at the maximum negative moment region, parallel to the support line and then diagonal cracks originated from each corner of the cutout. As the load was increased, additional flexural cracks formed and became wider, especially the main diagonal cracks from each corner of the cutout as shown in Fig. 6.

3.2 Rupture of CFRP Sheets

Failure mode of the strengthened slabs S3 and S4 was mainly due to the rupture in the CFRP sheets. However, the rupture was preceded by steel yielding. The load carrying capacity at failure was relatively larger for the CFRP strengthened slabs. No significant differences in crack patterns between strengthened and un-strengthened slabs was

Table 4 Ultimate loads and failure modes of tested slabs.

Group	Specimen	Ultimate load (kN)	Failure mode
Reference	S0	67	Flexure
1	S1	56	Flexure
	S2	41	Flexure
2	S3	62	Rupture of CFRP sheets
	S4	45	Rupture of CFRP sheets

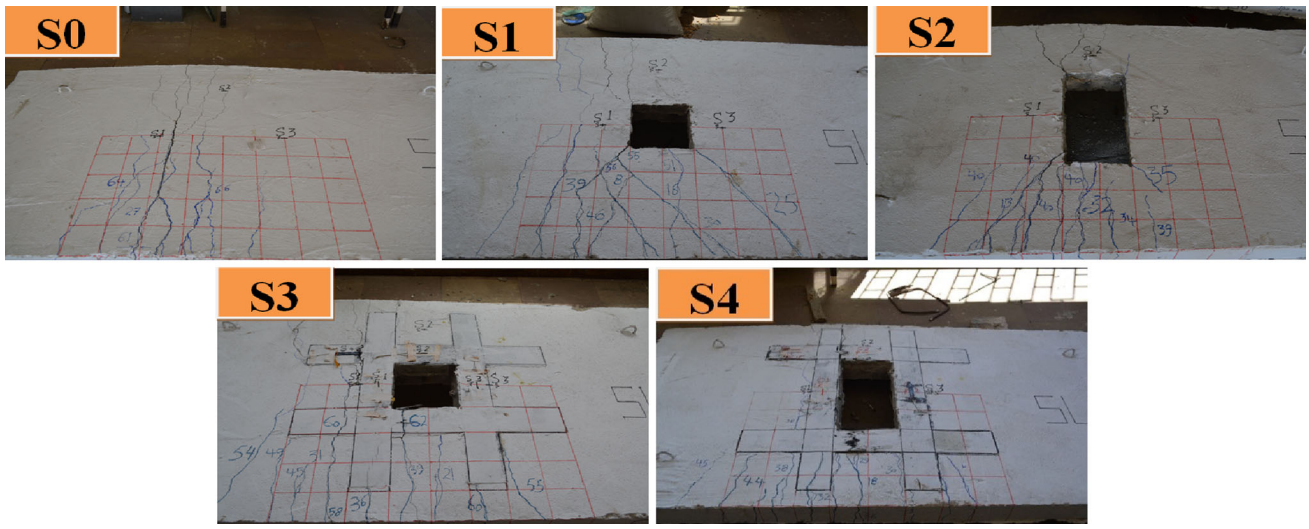

Fig. 6 Crack patterns of tested slabs.

observed, the extent of cracking from the corners of the cutout to the slab edges become not wider in strengthened slabs.

3.3 Behavior of Tested Slabs

Based on the experimental results, the behavior of the tested slabs is discussed in terms of observed crack patterns, ultimate load, measured deflection, and measured strains at different locations along the reinforcing steel bars, concrete surface, and CFRP sheets. The relationships between the applied load, deflection, and the longitudinal strains for concrete, steel, and CFRP of the tested slabs were typical for all tested slabs. Linear behavior followed by a nonlinear Trend and strain hardening and softening until failure. The slope of the first part of the plotted curves (load vs strain) of the tested slabs showed expected behavior until reaching 30 kN (where cutout was made), after that being sharper for un-strengthened slabs, the slope decreases by strengthening the cutouts using CFRP sheets. The reference slab (S0) where no cutout was made showed higher point of initial cracking than the rest of all tested slabs due to the presence of cutout that reduces the slab stiffness.

The ultimate loads of slabs (S3) and (S4) increased by about 10.7 and 9.7%, compared to slabs (S1) and (S2), respectively. The strengthening of the cutouts using CFRP sheets showed higher ultimate load due to the confinement stresses provided by the CFRP sheets. The deflection of slabs (S3) and (S4) decreased by about 23 and 17% respectively compared to the deflection at failure loads for slabs (S1) and (S2), respectively as shown in Fig. 7. CFRP sheets reached the ultimate strain at failure load when the steel bars reached the ultimate strain before failure load due to the effect of strengthening application. The steel bars close to the cutout had been strained significantly; the strengthened slabs were strained less than the un-strengthened slabs due to the effect of the encirclement by CFRP laminates as shown in Fig. 8. Transverse CFRP laminates were strained proportionally with loading because of the diagonal cracks originated from each corner of the cutout as shown in Fig. 9.

4. Finite Element Analysis

4.1 Element Type and Meshing

The finite element (FE) code ANSYS (2011) was used in this study. The experimental results were used to calibrate the FE models. The FE used to extend the parametric study beyond the limited number of specimens performed experimentally. Finite element models of reinforced concrete structures have generally been based on mesh discretization of a continuous domain into a set of discrete subdomains, usually called elements representing the concrete and the steel reinforcement. In this study, the discrete element approach was used to simulate reinforcement, where the reinforcement is modelled using beam elements connected to the concrete at certain shared mesh nodes as shown in Fig. 10. Also, since the reinforcement is superimposed in the concrete mesh, concrete exists in the same regions occupied by the reinforcement. The drawback of using the discrete model is that the concrete mesh is restricted by the location of the reinforcement. Full bond is generally assumed between the reinforcement and the concrete.

Concrete and resin was modeled using 3D 8-node solid elements (SOLID65). The main feature of this element is the ability to account for material nonlinearity. This element is capable of considering cracking in three perpendicular directions, plastic deformation and crushing, and creep. The element is defined by eight nodes having three translation degrees of freedom at each node in the x, y and z directions as shown in Fig. 11.

The SOLID185 element is used for modeling the steel plates and the CFRP composite. This element is defined by eight nodes having three degrees of freedom at each node; translations in the nodal x, y, and z directions. The element is capable of plasticity, hyper elasticity, stress stiffening, creep,

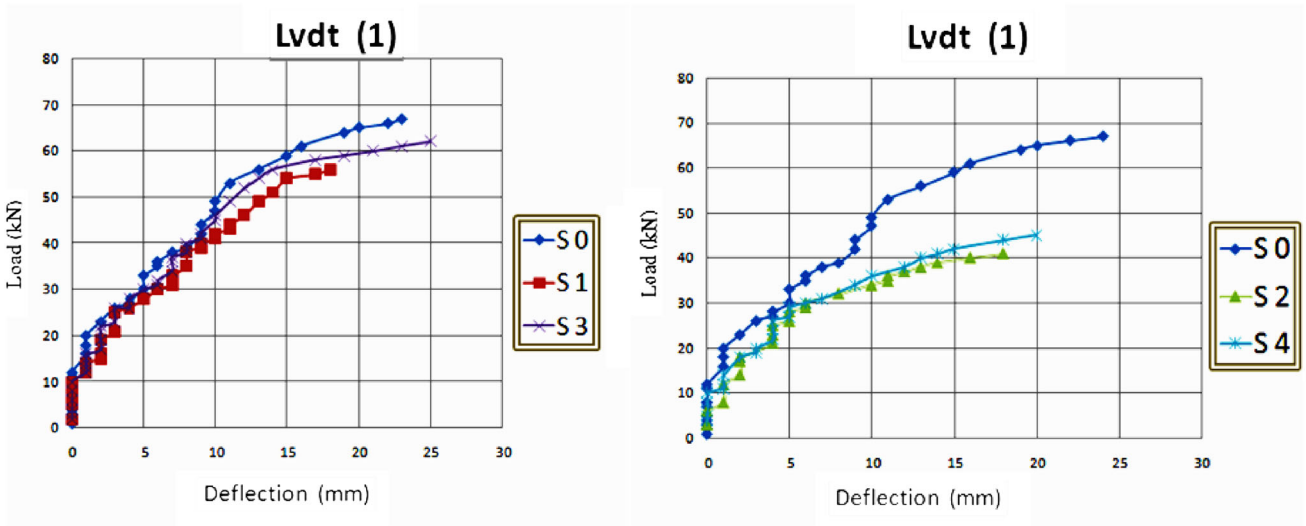

Fig. 7 Load-deflection curves for tested slabs.

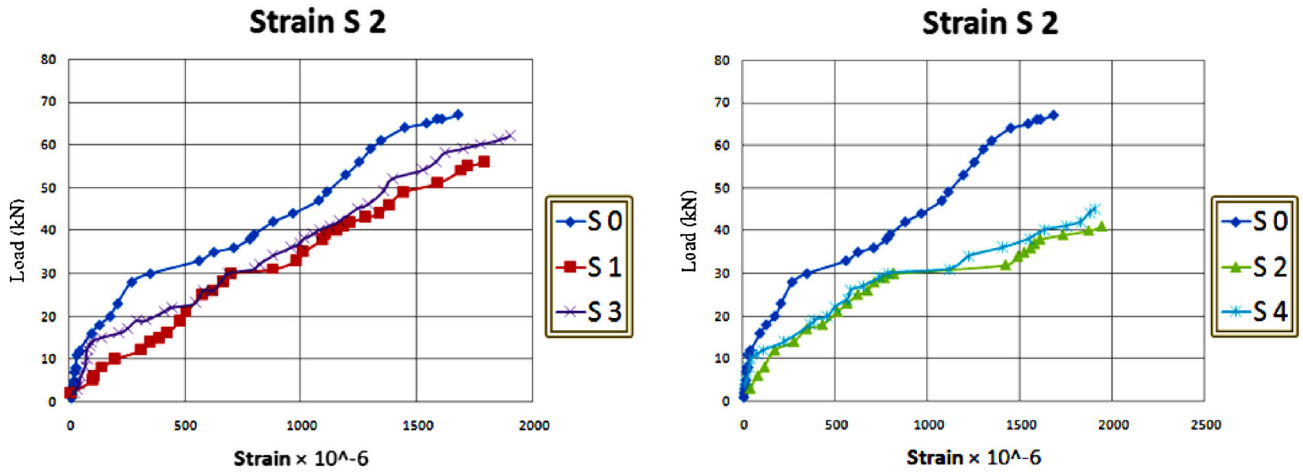

Fig. 8 Load-strain curves for steel bars of tested slabs.

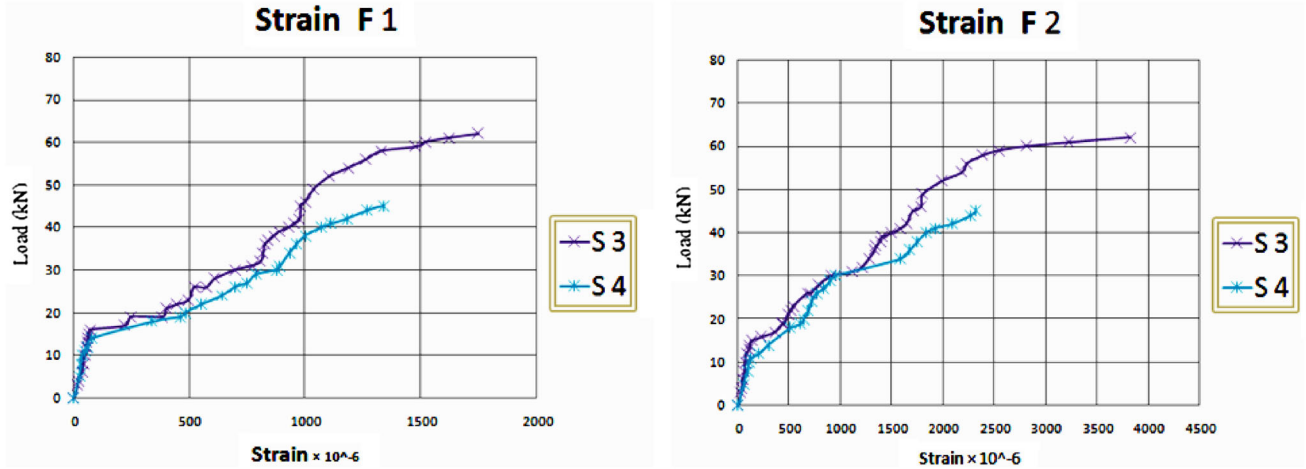

Fig. 9 Load-strain curves for CFRP sheets of strengthened slabs.

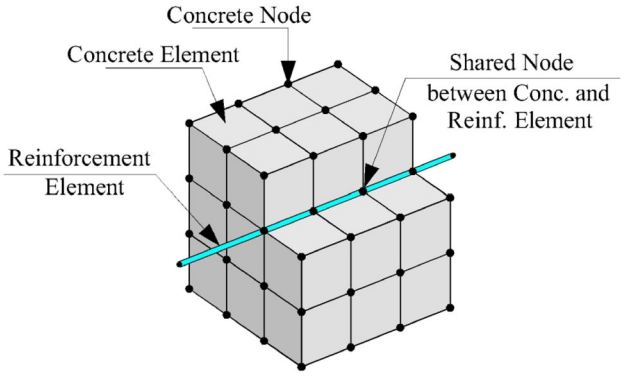

Fig. 10 Discrete model for reinforced concrete (ANSYS).

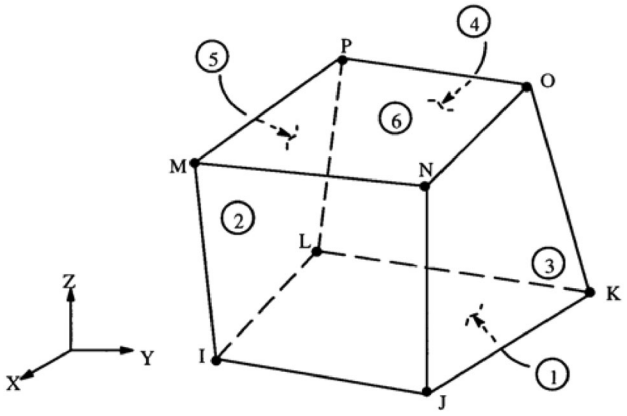

Fig. 11 SOLID 65 3D-reinforced concrete solid element, ANSYS (2011).

large deflection, and large strain capabilities. SOLID185 element uses enhanced strain formulation, simplified enhanced strain formulation, or uniform reduced integration. The SOLID185 in the form of homogeneous structural solid is used in this study to model the Carbon fiber and the steel plate as shown in Fig. 12.

A LINK180 element is used to model steel reinforcement. The element is a uniaxial tension–compression element with three degrees of freedom at each node: Translations in the nodal x, y, and z directions. This element is also capable of plastic deformation. Figure 13 shows the geometry of LINK180.

The properties of the FE elements depend on the element type such as cross-sectional area of beam element is known in ANSYS as real constants. Not all element types require real constants to be defined, and different elements of the same type may have different real constant values. In case of

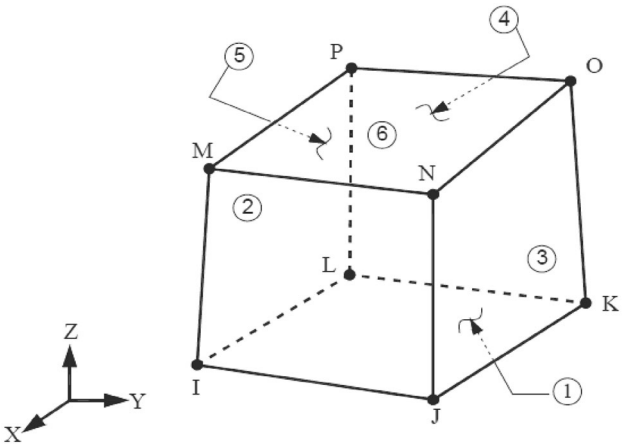

Fig. 12 SOLID185 3D- Homogeneous Structural solid element, ANSYS (2011).

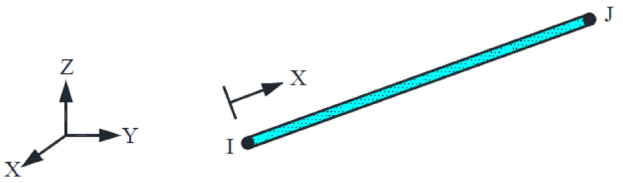

Fig. 13 LINK180 element geometry, ANSYS (2011).

concrete, real constants defined only for SOLID65 element and in the present study the concrete is modeled using discrete reinforcement. Therefore, all real constants which activate the smeared reinforcement are disabled by putting it equal to zero. As there are no reinforcements through the resin, then, the same real constants are specified to the SOLID65 element for resin. In general, crushing stiffness factor (CSTIF) for concrete is set to be 0.1. SOLID185 in form of homogeneous Structural Solid or layered Structural Solid does not require the definition of real constants. LINK180 has real constants; cross sectional area, and added mass (mass/length). Both tension and compression capability is chosen.

4.2 Concrete

In modern fracture mechanics concrete is considered as a quasi-brittle material, that's where the stress decreases gradually after the peak stress, and the properties of concrete in compression and tension are different from each other. The tensile strength of concrete is typically 8–15% of the compressive strength. Figure 14 shows a typical stress–strain curve for normal weight concrete according to Bangash (Mota and Kamara 2006).

As shown in Fig. 14, when concrete subjected to compression load, the stress–strain starts linearly in an elastic manner up to about 30 percent of the maximum compressive strength σ_{cu}, then, the stress increases gradually up to the maximum compressive strength, and then, the curve descends into a softening region, and eventually crushing failure occurs at an ultimate strain ε_{cu}. In tension zone, the stress strain curve is approximately linearly elastic up to the

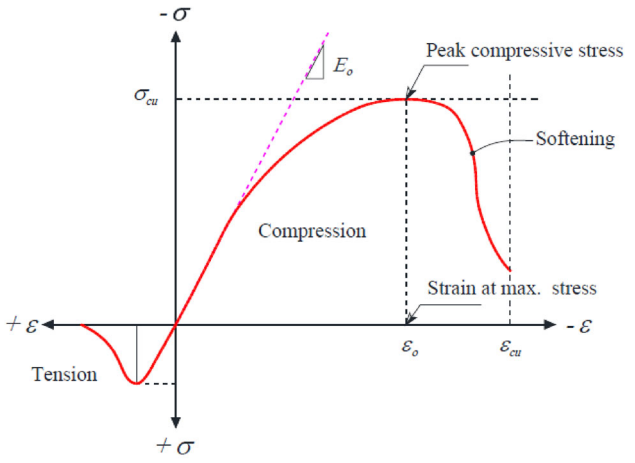

Fig. 14 Typical Uniaxial Compressive and Tensile Stress–Strain Curve for Concrete, Bangash, (Mota and Kamara 2006).

maximum tensile strength. After this point, the concrete cracks and the strength decreases gradually to zero.

Typical shear transfer coefficients range from (0.0 to 1.0), with 0.0 representing a smooth crack (complete loss of shear transfer) and 1.0 representing a rough crack (no loss of shear transfer). This specification may be made for both the closed and open crack. When the element is cracked or crushed, a small amount of stiffness is added to the element for numerical stability. The stiffness multiplier CSTF is used across a cracked face or for a crushed element to be equal to 0.1, ANSYS 2011 (ANSYS 2011). A number of preliminary analyses were attempted in this study with various values for βt and βc within a range between (0.15 to 0.9) and (0.5 to 0.9) respectively. Where βt and βc are shear transfer coefficient for open cracks (βt), and shear transfer coefficient for closed cracks (βc), (ANSYS 2011). For this analysis βt and βc were set to 0.2 and 0.8 respectively, achieving a good converging problem. The uniaxial cracking strength is taken to be equal to the modulus of rupture of concrete. Due to the similarity of resin with concrete in its behavior toward the tensile and compression stress, so SOLID65 solid element with linear and nonlinear properties is used to represent the resin in the present model.

4.3 FRP Composites

The FRP composites are anisotropic materials; where the material properties are different in all directions. For the unidirectional lamina, it has three mutually orthogonal planes of material properties, (xy, xz, and yz planes). The xyz coordinate axes are referred to as the principal material coordinates where the x-direction is the same as the fiber direction, and the y and z directions are perpendicular to the x direction. It is a so-called especially orthotropic material. The perpendicular plane of fiber direction can be considered as isotropic material, that's where; the properties in the y-direction are the same as those in the z-direction. FRP laminates have stress–strain relationships that are roughly linear up to failure. In the nonlinear analysis of the full-scale transverse slabs, no FRP elements show stresses higher than

their ultimate strengths. Consequently, in this study it is assumed that the stress strain relationships for the FRP laminates are linearly elastic.

4.4 Steel Reinforcement

The reinforcement element was assumed to be a bilinear isotropic elastic-perfectly plastic material and identical in tension and compression as shown in Fig. 15. Poisson's ratio of 0.3 was used for all types of steel reinforcement.

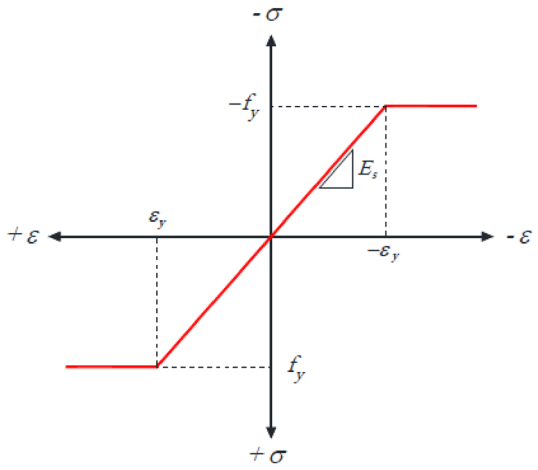

Fig. 15 Stress-strain curve for steel reinforcement.

4.5 Loads and Boundary Conditions

The bond between concrete and steel is assumed to be perfect, and poisson's ratio is assumed to be constant throughout the loading steps. Time-dependent nonlinearities such as creep, shrinkage, and temperature change are not included in this study. Concrete damaged plasticity model in ANSYS provides a general capability for modeling concrete. It uses the concepts of isotropic damaged elasticity and isotropic tensile and compressive plasticity to represent concrete inelastic behavior. To ensure that the model acts the same way as the experimental slabs, boundary conditions were applied at two supports (steel plates have 20 mm thickness, 50 mm width and 1000 mm long) which located under slabs to prevent local cracking in concrete, The nodal displacement load is used to model the boundary condition in this ANSYS models, The hinged support was created by putting the value of the displacement DOFs for X, Y and Z directions to be equal zero, consequently and the roller support was created by putting the value of the displacement DOFs for Y and Z directions to be equal zero, consequently. The load was applied as line load in Y direction.uniformly in Z direction in two positions. All slabs were loaded up to (30 KN) load then restart analysis for producing cut out by killing elements, after that operation the slabs were loaded till failure. Figure 16 shows the FE models of two of the specimens. The FE model of the studied slabs with and without opening is shown in Fig. 16.

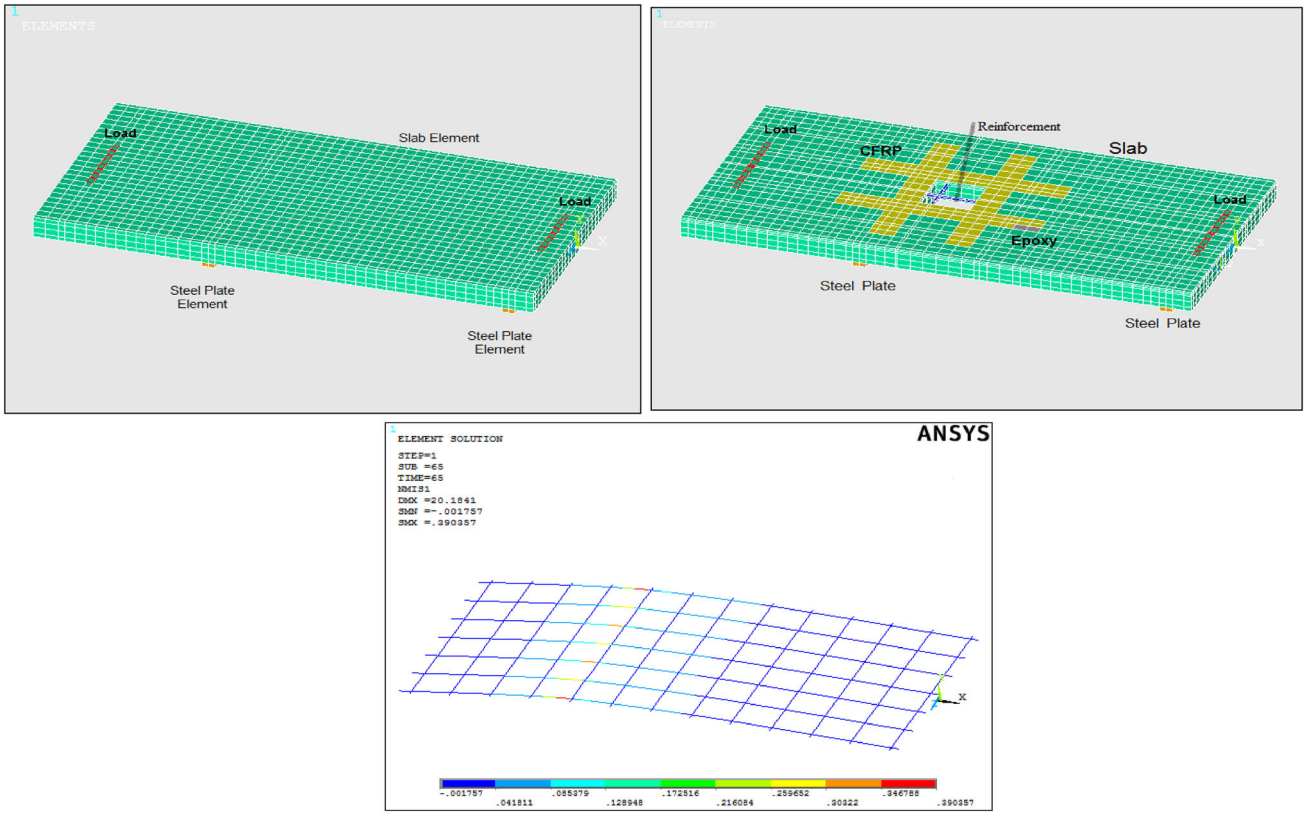

Fig. 16 FE model of the control slab, slab (1), and reinforcement mesh.

Table 5 Comparison between experimental and finite element results.

Group	Specimen	Experimental ultimate load pue (kN)	Finite element ultimate load P_{uf} (kN)	P_{uf}/P_{ue}
Reference	S0	67	65	0.97
1	S1	56	55.2	0.99
	S2	41	42	1.02
2	S3	62	60	0.97
	S4	45	45.8	1.02

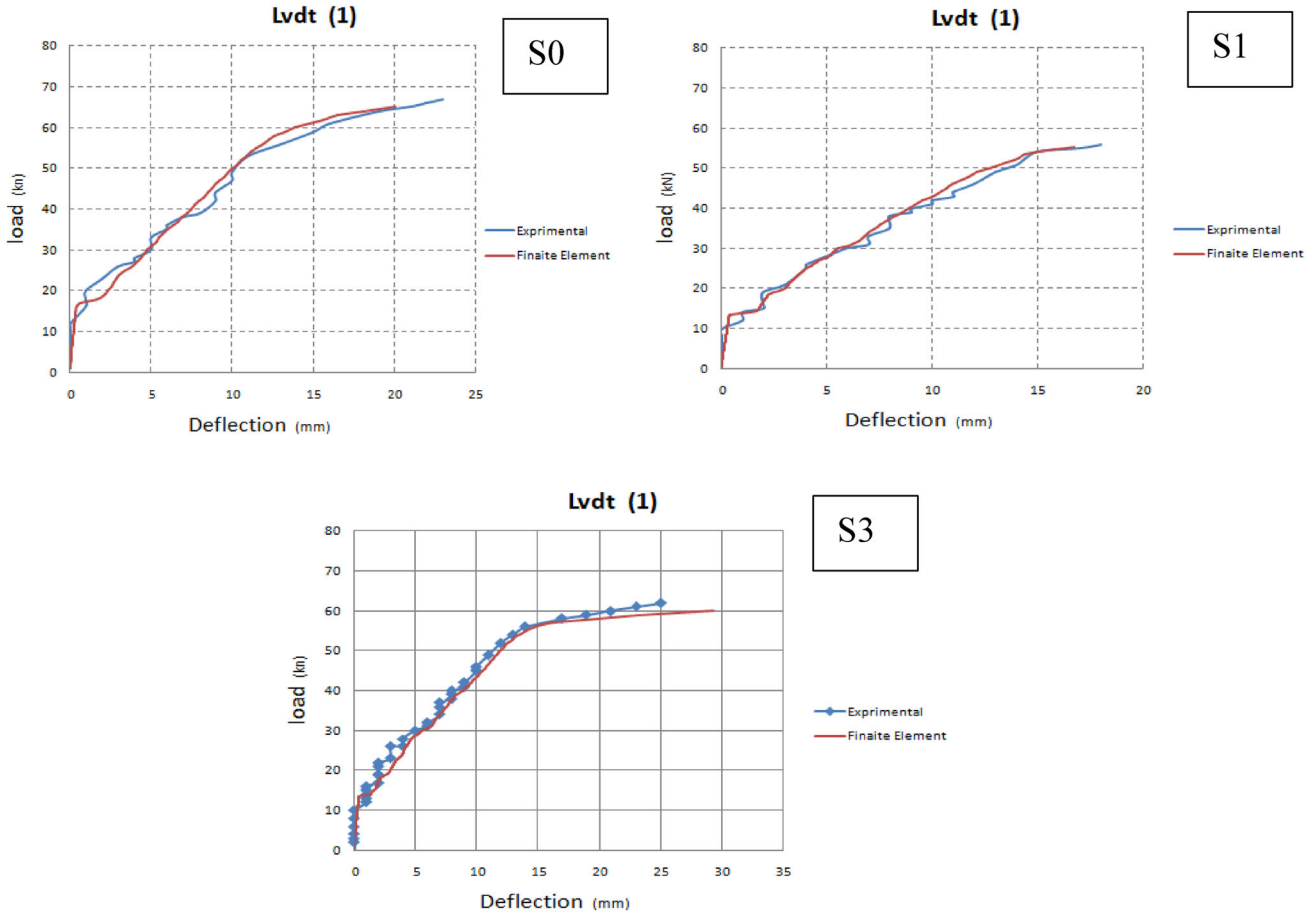

Fig. 17 Load-displacement history of slabs S0, S1, and S3.

5. Comparison Between FE and Experimental Results

The finite element results were compared to the experimental results obtained previously. The results were found to be in good agreement, therefore the finite element test program is extended further beyond the experimental cases to investigate the behavior of more slabs. Table 5 shows the ultimate loads from the FE model and the experiments. Figure 17 shows the load–displacement history of slabs S0, S1, and S3, it can be shown that the differences in the results are in very good agreement with a percentage of error of ±3%. The obtained results showed that the FE model could be used for further slab cases (Fig. 18).

More cases were considered by studying the effect of number of CFRP layers and laminates areas as shown in Table 6. The CFRP layers width increased from 100 to 200 mm, where the CFRP area was increased from 13 to 130 mm^2 as a function of the number of layers. As expected, Increasing the cross sectional area of CFRP by 100%, led to an increase in the ultimate load 0f 14.1% for one layer. Figure 19 shows the effect of number of layers on the ultimate slab load. In general, increasing the number of CFRP layers, has a significant increase in the ultimate load.

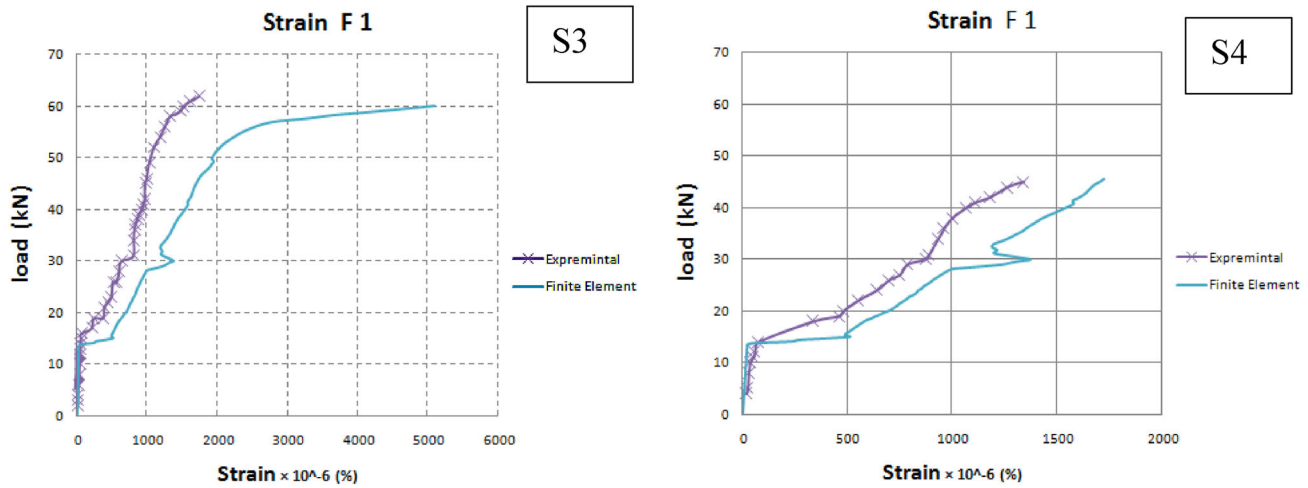

Fig. 18 Load-strain history in the longitudinal direction (F1) of slabs S3 and S4.

Table 6 Effect of increasing CFRP number of layers and widths on ultimate loads.

Model	Cutout size, mm	No. of layers	Layer width, mm	Area of CFRP layers, mm^2	Ultimate load (kN)	% increase ultimate load
S1	200 × 200	–	–	–	55.2	–
S2	200 × 400	–	–	–	42.0	–
S3	200 × 200	1	100	13.0	60.0	8.7
			150	19.5	62.4	13.0
			200	26.0	63.0	14.1
		2	100	26.0	63.0	14.1
			150	39.0	65.2	18.1
			200	52.0	67.2	21.7
		3	100	39.0	64.8	17.4
			150	58.5	69.0	25.0
			200	78.0	71.4	29.3
S4	200 × 400	1	100	13.0	45.8	9.0
			150	19.5	47.4	12.9
			200	26.0	48.6	15.7
		2	100	26.0	49.2	17.1
			150	39.0	51.6	22.9
			200	52.0	52.8	25.7
		3	100	39.0	51.6	22.9
			150	58.5	54.6	30.0
			200	78.0	57.6	37.1
		4	100	52	53.4	27.1
			150	78	58.2	38.6
			200	104.0	64.2	52.9
		5	100	65.0	56.4	34.3
			150	97.5	63.0	50.0
			200	130.0	69.0	64.3

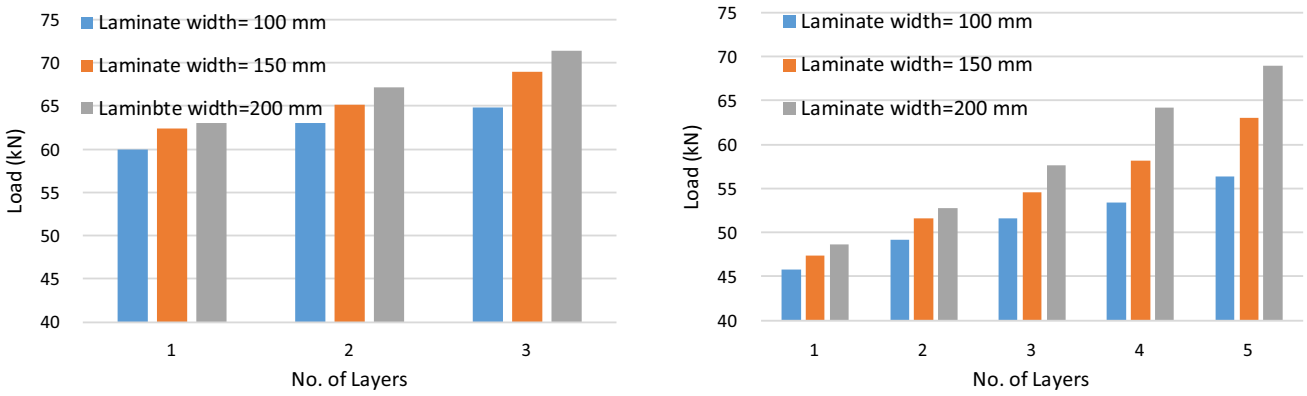

Fig. 19 Effect of CFRP layers for slab groups 1 (*left*) and 2 (*right*).

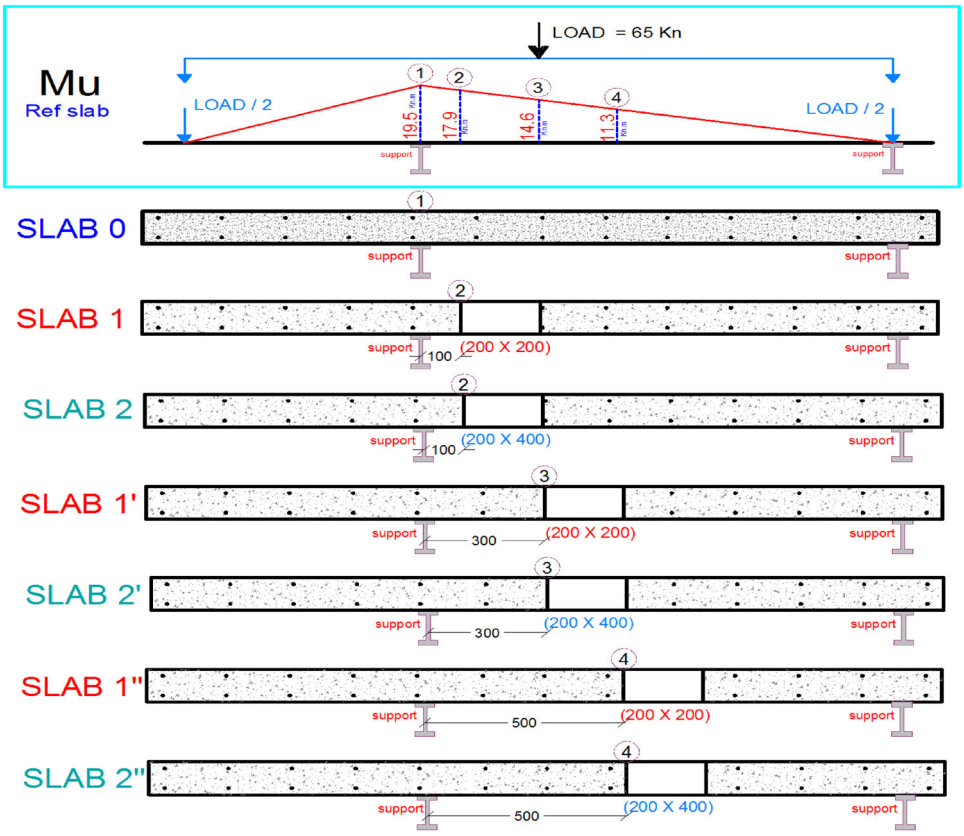

Fig. 20 Position of cutouts in hogging region, quarter and mid span.

5.1 Calculations of CFRP Amount Required for Strengthening

According to the results listed in Table 6. The amount of CFRP used to strengthen slabs was computed under the premise that the loss of steel reinforcement caused by the cutout would be replaced by an equivalent amount of CFRP to restore the load carrying capacity of R.C. slabs after having cut out according to the following simple relationship.

$$Es\,As_{lost} = Ef\,Af \tag{1}$$

The amount of steel reinforcement lost is equivalent to:

$$A_{s\,lost} = N \times A \tag{2}$$

where (N) is the number of steel bars which have been cut we can compute the equivalent area of CFRP for each side direction.

$$A_{CFRP} = \frac{E_s}{E_{CFRP}} \times \frac{1}{2} A_{slost} \tag{3}$$

Since each layer has a width (b CFRP), the necessary overall thickness of CFRP laminate is given by:

$$T_{total} = \frac{A_{CFRP}}{b_{CFRP}} \tag{4}$$

Table 7 Effect of changing cutouts positions on ultimate load.

Section	Location	Model	Ultimate load, P_u (kN)	$P_u/P_{u\ (s0)}$	Moment of resistance M_r (kN m)	Ult.Ld. after strengthening, P_u (kN)	% increase ultimate load
1	At support (M1 = 19.5 kN m)	S0	65.0	1.00	19.0	Reference	–
2	Hogging zone (M2 = 17.9 kN m)	S1	55.2	0.85	16.0	S3 = 60.0	8.7
		S2	42.0	0.65	11.7	S4 = 45.8	9.0
3	Quarter span (M3 = 14.6 kN m)	S1′	63.0	0.97	16.0	S3′ = 63.6	1.0
		S2′	55.0	0.85	11.7	S4′ = 59.4	8.0
4	Mid span (M4 = 11.3 kN m)	S1″	64.2	0.99	16.0	S3″ = 64.8	1.0
		S2″	63.6	0.98	11.7	S4″ = 64.2	1.0

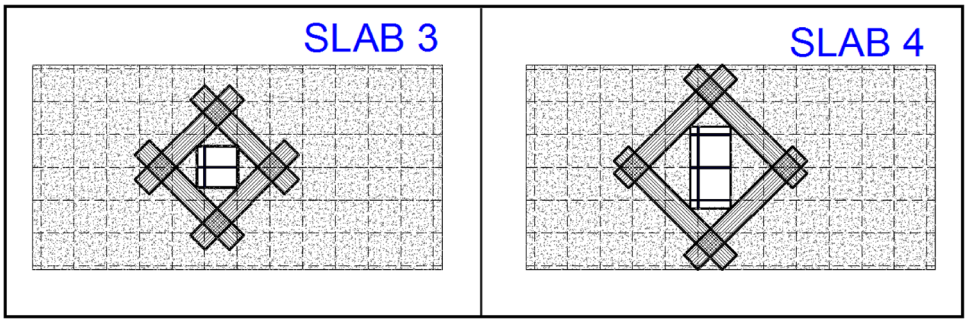

Fig. 21 Strengthened slabs with CFRP sheets with 45°.

Table 8 Effect of changing CFRP sheets configuration around cutouts on ultimate load.

Model	CFRP sheets configuration around cutout	Ultimate load (kN)	% increase ultimate load
S1	–	55.2	–
S3	Parallel to cutout edges	60.0	8.7
	Inclined 45° at cutout corners	57.0	3.2
S4	Parallel to cutout edges	45.8	9.0
	Inclined 45° at cutout corners	43.4	3.3

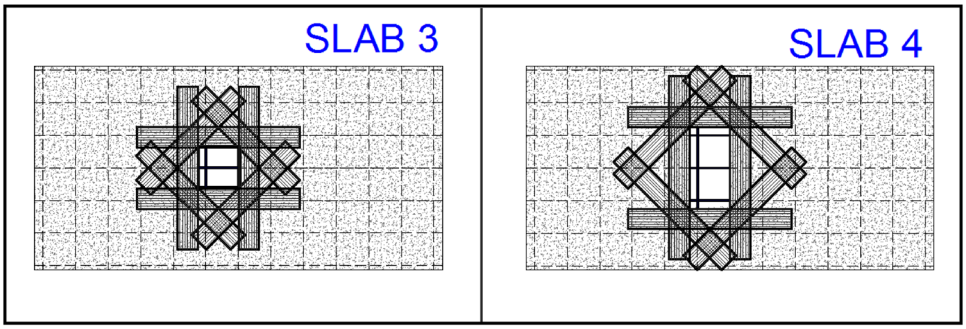

Fig. 22 Strengthened Slabs with CFRP sheets with 90°and 45°.

Given that thickness of one layer = 0.13 mm, the total number of layers required is:

$$\text{No.of layers} = \frac{T_{\text{total}}}{0.013\ \text{mm}} \tag{5}$$

For group 1, (N = 1) is the number of steel bars which have been cut (for slab with opening 100 * 100 mm). Substituting into Eq. (3) we can compute the equivalent area of CFR = 33.3 mm^2. For group 2 (N = 3) is the number of steel bars which have been cut (for slab with opening

200 * 100 mm). Substituting into Eq. (3) we can compute the equivalent area of CFRP = 100 mm^2.

5.2 Effect of Cutouts Location

Further FEA study has been considered in this section, by investigating the slab behavior based on the cutout location. All slabs in this parametric study had the same properties, dimensions, cutouts dimensions, reinforcement and boundary conditions as slabs which tested experimentally. The cutout location was measured from the intermediate support toward the simply supported edge as shown in Fig. 20. The cutout was considered at hogging moment region, 200 and 500 mm from the intermediate support incorporated by the cutout sizes (200 × 200 and 200 × 400 mm).

It can be seen form Table 7 that locating the cutout at the hogging zone (S2), increased the ultimate load by 9% compared to the control slab. Whereas locating the cutout at the mid span did not have any significant effect on the load carrying capacity of the tested slabs.

5.3 Effect of Changing of CFRP Configurations Around Cutouts

The effect of changing the CFRP configurations has been studied as well. The CFRP has been assumed at 45° around the cutout for slabs S3 and S4 as shown in Fig. 21.

From Table 8, Slabs strengthened with CFRP sheets along the cutout edges (90°) give results higher than the cases where CFRP sheets are inclined by 45° with respect to the cutout corners. In case of strengthening with 90° and 45° will get the highest load carrying capacity due to the crack propagation is hindered by three layers of CFRP sheets as shown in Fig. 22.

6. Conclusions

1. The relationships between the applied load, deflection, and the longitudinal strains for concrete, steel, and CFRP of the tested slabs were typical for all tested slabs, a linear increase behavior followed by a nonlinear behavior until failure has been observed.
2. The slope of the first part of the axial load-strain curves of the tested slabs showed the expected trend and behavior until reaching 30 kN loading (producing cut out), after that the slope became sharper for un-strengthened slabs, the sharpness degree decreased by strengthening the slabs by CFRP sheets.
3. The ultimate loads increased by about 10.7 and 9.7% for slab groups 1 and 2, respectively when slabs strengthened using CFRP sheets and that is due to the confinement stress provided by the CFRP sheets. The deflection decreased by about 23 and 17% for slab groups 1 and 2, respectively when slabs strengthened using CFRP sheets.
4. Reference and un-strengthened slabs had flexural mode failure, where the steel bars reached the ultimate strain at failure load. For strengthened slabs, the rupture of CFRP sheets was the control mode of failure, the CFRP sheets reached the ultimate strain at failure load when the steel bars reached the ultimate strain before failure load due to strengthening technique.
5. The steel bars beside cutout directly had been strained significantly; the strengthened slabs had strained less than the un-strengthened slabs due to the effect of the encirclement by CFRP laminates, whereas transverse CFRP laminates strained proportionally with loading although it was parallel to load line but the practical reason was the diagonal cracks originated from each corner of the cutout.
6. The finite element model results closely agreed with the experimental results; the model overestimates the values of the ultimate loads of the tested slabs by 2–3%.
7. The amount of CFRP used to strengthen slabs was computed under the premise that the loss of steel reinforcement caused by the cutout would be replaced by an equivalent amount of CFRP to restore the load carrying capacity of R.C. slabs after having cutout.
8. To select suitable cutout location in existing R.C. slabs, the moment of resistance should be considered for slab at cutout's section. The position of the cutout with CFRP strengthening doesn't provide significant change in load capacity, and finally slabs strengthened with CFRP sheets along the cutout edges give results higher than CFRP sheets at the cutout's corners with 45° only.

Open Access

References

ACI 318-14, "Building Code Requirements for Structural Concrete and Commentary", American Concrete Institute, Farmington Hills, Michigan, February, 68 pp.

ANSYS. (2011). *Release 14.0 documentation*. ANSYS Inc. http://www.ansys.com

Casadei, P., Nanni, A., & Ibell, T. J. (2003). Experiments on two-way RC slabs with openings strengthened with CFRP laminates. In *Proceedings of advancing with composites, PLAST 2003*. Milan, Italy, Conference 7–9 May, Conference 2003.

Enochsson, O., Lundqvist, J., Taljsten, B., Rusinowski, P., & Olofsson, T. (2007). CFRP strengthened openings in two-way concrete slabs—An experimental and numerical study. *Construction and Building Materials, 21*(4), 810–826.

Khajehdehia, R., & Panahshahib, N. (2016). Effect of openings on in-plane structural behavior of reinforced concrete floor slabs. *Journal of Building Engineering, 7*, 1–11

Mosallam, A. S., & Mosalam, K. M. (2003). Strengthening of two-way concrete slabs with FRP composite laminates. *Construction and Building Materials, 17,* 43–54.

Mota, M. C., & Kamara, M. (2006). Floor openings in two-way slabs. *Concrete Int., 28*(7), 33–36.

Muhammed, N. (2012). Experimental study of self compacting RC slabs with opening strengthening with carbon fiber laminated and steel fiber. *Journal of Engineering and Development, 16*(1), March 2012 ISSN 1813-7822.

Ozgür, A., Nalan, K., & Onur, A. (2013). Strengthening of one way RC slab with opening using CFRP strips. *Construction and Building Materials, 48*(10), 883–893.

Smith, S. T., & Kim, S. J. (2009). Strengthening of one-way spanning RC slabs with cutouts using FRP composites. *Construction and Building Materials, 23,* 1578–1590.

Song, J. K., Kim, J., Song, H. B., & Song, J. W. (2012). Effective punching shear and moment capacity of flat plate-column connection with shear reinforcements for lateral loading. *International Journal of Concrete Structures and Materials., 6*(1), 19–29.

Sorin-Codrut, F., Sas, G., Popescu, C., & Stoian, V. (2015). Tests on reinforced concrete slabs with cut-out openings strengthened with fibre-reinforced polymers. *Composites: Part B, 66,* 484–493.

Tan, K. H., & Zhao, H. (2004). Strengthening of openings in one-way reinforced-concrete slabs using carbon fiber-reinforced polymer systems. *J Compos Constr, 8*(5), 393–402.

Vasquez, A., & Karbhari, V. M. (2003). Fiber-reinforced polymer composite strengthening of concrete slabs with cutouts. *ACI Struct J, 100*(5), 665–667.